Available online at www.sciencedirect.com

SCIENCE DIRECT

Materials Letters 58 (2004) 3765–3768

materials letters

www.elsevier.com/locate/matlet

Optical properties of Ge/Si quantum dot superlattices

Zheng Yang[a,*], Yi Shi[a], Jianlin Liu[b], Bo Yan[a], Rong Zhang[a], Youdou Zheng[a], Kanglong Wang[c]

[a]Department of Physics and National Laboratory of Solid State Microstructures, Nanjing University, Nanjing 210093, China
[b]Department of Electrical Engineering, University of California at Riverside, Riverside, CA 92521, USA
[c]Department of Electrical Engineering, University of California at Los Angeles, Los Angeles, CA 90095, USA

Received 24 February 2004; received in revised form 30 July 2004; accepted 12 August 2004
Available online 11 September 2004

Abstract

Self-assembled Ge/Si quantum dot (QD) superlattices (SLs) were grown by a solid-source molecular beam epitaxy (MBE) system with the Stranski-Kranstanov (SK) growth mode. Atomic force microscope (AFM) and transmission electron microscope (TEM) characterizations of the samples were presented. Photoluminescence (PL) and Raman scattering measurements were carried out. The temperature dependence of the PL intensity has been reported and fitted by the Arrhenius and Berthelot type function. Some valuable parameters were obtained through the fitted curves, one of which was closely related to the dimension and effective mass of electron of the QDs.
© 2004 Elsevier B.V. All rights reserved.

PACS: 78.67.−n; 81.07.Ta; 78.67.Pt; 81.15.Hi; 78.55.−m; 78.30.−j
Keywords: Optical properties; Quantum dots; Superlattices; Photoluminescence; Raman scattering; MBE

1. Introduction

Self-assembled QDs by the SK growth mode and QD SLs have attracted a great deal of attention for several years, both for their fundamental physics study and potential applications in fabricating novel devices. Recent study showed that some QD SLs could be fabricated as thermoelectric devices with high performance [1] and Ge QDs might be used in several valuable areas, such as nanoelectronics, optoelectronics, and thermoelectrics [2]. To study the optical properties in Ge QDs is indispensable before their real applications. In this letter, we reported the study of PL and Raman scattering in self-assembled Ge QD SLs, from which we can study the electron and phonon transport in such low-dimensional nanostructures.

* Corresponding author. Tel.: +86 25 8445 9351; fax: +86 25 83596225.
E-mail addresses: yangzenith@263.net (Z. Yang), yshi@nju.edu.cn (Y. Shi).

0167-577X/$ - see front matter © 2004 Elsevier B.V. All rights reserved.
doi:10.1016/j.matlet.2004.08.016

2. Experimental results and discussion

2.1. Growth

Three samples, labeled A to C, were grown on (100)-oriented Si substrates covered by 100 nm buffer layer, using a solid-source MBE system with the SK growth mode. The samples consist of some period bilayers, in which Ge layers were separated by 20-nm-thick Si spacer layers. The Ge layer thickness of sample B was 1.2 nm, while those of samples A and C were both 1.5 nm. Samples A, B, and C were consisted of 35, 10, and 20 periods of Ge/Si bilayers, respetively. The growth temperature was 540 °C. The uniformity, shape and the degree of Si/Ge interdiffusion of the samples are influenced by the growth temperature [3]. The growth parameters and structural data of the samples were summarized in Table 1.

Fig. 1(a) and (b) show the two- and three-dimensional AFM image of sample A. The Ge layer nominal thickness is 1.5 nm and the Si spacer layer thickness is 20 nm. The dots are all dome-shaped with the base size and the height of about 100 and 15 nm, respectively. Fig. 2

Table 1
Growth parameters and structural data of the three samples

Sample	Ge layer thickness (nm)	Si layer thickness (nm)	Growth temperature (°C)	Periods
A	1.5	20	540	35
B	1.2	20	540	10
C	1.5	20	540	20

shows the cross-sectional TEM image of sample B—a 10-period self-assembled Ge QD SL sample grown at 540 °C. The Ge layer nominal thickness is 1.2 nm and the Si spacer layer thickness is 20 nm. Vertically correlated islands are evident. The origin of vertical correlation is attributed to preferential nucleation due to the inhomogeneous strain field induced by buried dots.

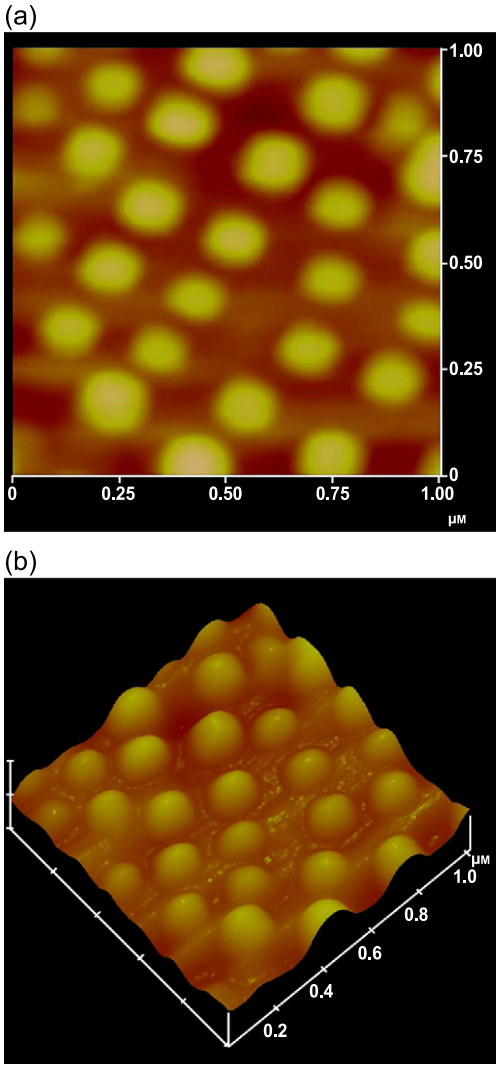

Fig. 1. (a) Two-dimensional (2D) and (b) three-dimensional (3D) AFM images of a uniform self-assembled Ge/Si quantum dots sample at the growth temperature of 540 °C. The thickness of Ge and Si spacer layer were 1.5 and 20 nm, respectively.

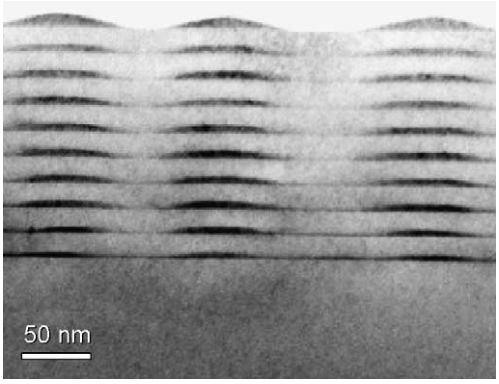

Fig. 2. Cross-sectional TEM image of a 10-period self-assembled Ge/Si quantum dot superlattice sample. The growth temperature was 540 °C. The thickness of Ge and Si spacer layer were 1.2 and 20 nm, respectively. Vertical correlation was clearly seen.

2.2. Photoluminescence

Photoluminescence measurements were carried out in sample C—a 20-period self-assembled Ge QD SL sample. The growth temperature was 540 °C. The thickness of Ge and Si spacer layer were 1.5 and 20 nm, respectively. Fig. 3 shows the PL spectrum. The measurements were performed at 10 K. The strong peak centered around 1.1 eV is the Si transverse optical (TO) phonon assisted recombination. The peak located at higher energy than Si TO peak arises from other recombination in Si, such as Si transverse acoustic (TA) peak and Si no-phonon (NP) peak. The broad peaks at lower energies (from 0.7 to 1.0 eV) labeled "Ge dots" (inside the dashed-line rectangle) were attributed to electron-hole recombination within the dots or at the interface between the dots and surrounding Si [4,7]. These peaks can be decomposed into two peaks which correspond to NP-and TO-phonon assisted recombination [5,6]. The peaks between the Si TO-peak and the broad Ge dot peak arise

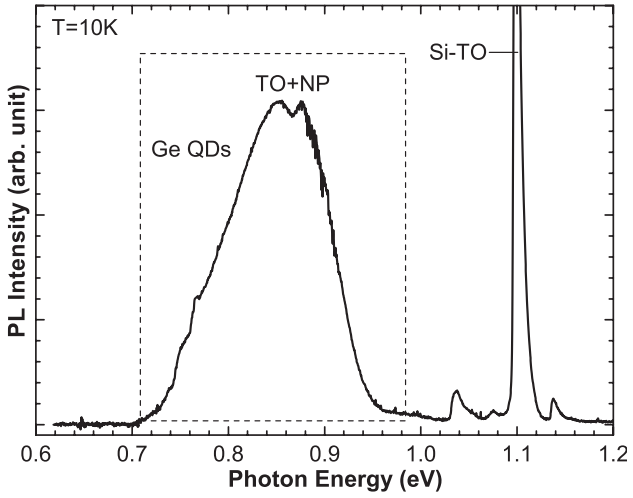

Fig. 3. PL spectrum of a 20-period self-assembled Ge/Si quantum dot superlattice sample. The growth temperature was 540 °C. The thickness of Ge and Si spacer layer were 1.5 and 20 nm, respectively.

from the Ge wetting layer. PL study has provided some insight about the band structure of the sample [5,6]. The frequency shift of the Ge dot peak can be used to estimate the degree of Si/Ge intermixing.

The temperature dependent PL spectra are presented in Fig. 4. The sample is the same as the one in Fig. 3. The PL curves of the sample were recorded at 10, 30, 50, 80, 120, 160 and 200 K. It has been reported that the temperature dependence of the PL intensity in nanocrystalline semiconductors is of the combination of Arrhenius and Berthelot type temperature dependence both in theoretical works [8a] and silicon clusters [8b]. We found that this rule also exist in the Ge/Si QDs. The temperature dependence of the PL intensity is given by Ref. [8]

$$\frac{I(T)}{I_0} = \frac{1}{1 + \upsilon \cdot \exp\left(\frac{T}{T_B} + \frac{T_r}{T}\right)}$$

where υ is characteristic reduced frequency and T_B and T_r are characteristic temperatures. In our experiments, $I(T)$ and I_0 are the integrated PL intensity at temperature T and 10 K, respectively.

Our experimental data were fitted using this model and the results are represented in Fig. 5., which is the temperature dependence of the PL intensity. The dots are the experimental data and the solid line is the fitted curves. In our fitted curve, the characteristic parameters T_B, T_r, and υ are equal to 31.6, 0, and 0.025 K, respectively. There is no contribution of the radiative term in this fitted curve. The characteristic temperature T_B is given by the expression [8]

$$T_B = \frac{\hbar^2}{2\pi^2 a^2 m_e^* k_B}$$

where a is the confinement size of the QD and m_e^* is the effective mass of the electron in the QD. The average height

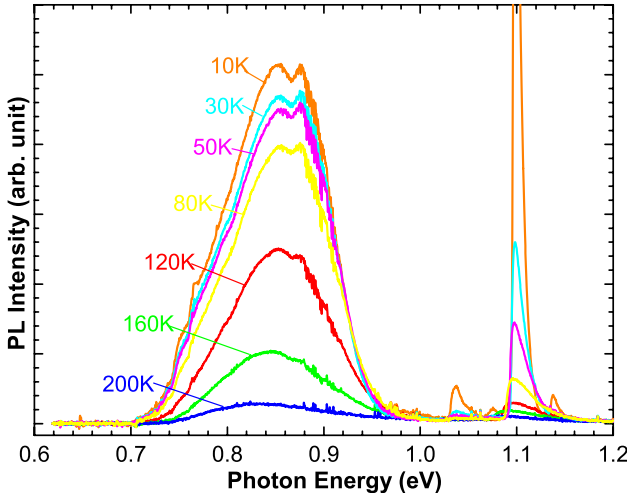

Fig. 4. Temperature dependent PL spectra of the same sample in Fig. 3. The PL curves were recorded at 10, 30, 50, 80, 120, 160 and 200 K.

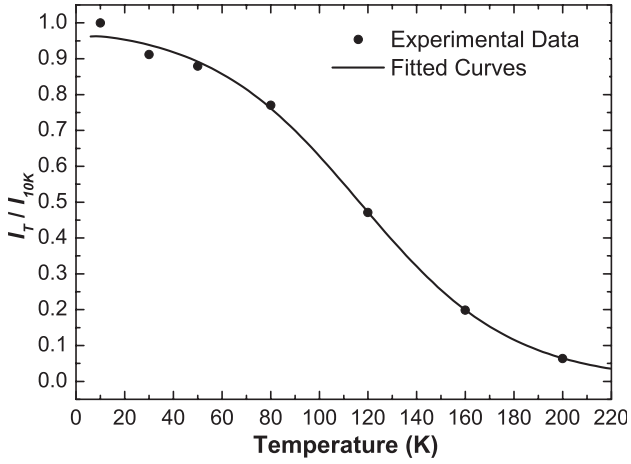

Fig. 5. The temperature dependence of the PL intensity. The dots are the experimental data. The solid line is the fitted curves.

of our QDs sample is about 10 nm, thus the m_e^* equals about 0.014 m_e, where m_e is the rest electron mass. The value of this effective mass can not be compared with that in bulk Ge, due to Si/Ge interdiffusion. Indeed, some Si have interdiffused into the QDs, which could be verified and estimated in the Raman scattering measurements.

2.3. Raman scattering

Raman scattering measurements were also carried out in sample C. Fig. 6 shows the Raman spectrum. The spectrum can be divided into two regions, i.e. the low frequency (<50 cm^{-1}) and normal frequency region, which are attributed to the acoustic and optical phonons in the samples, respectively.

In the normal frequency region, two obvious peaks were observed besides the strong Si substrate signal around 520

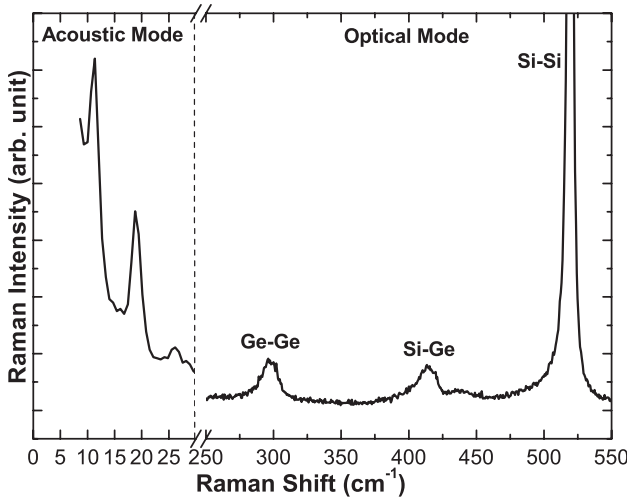

Fig. 6. Raman scattering spectrum of a 20-period self-assembled Ge/Si quantum dot superlattice sample. The growth temperature was 540 °C. The thickness of Ge and Si spacer layer were 1.5 and 20 nm, respectively.

cm^{-1}, which were Ge–Ge optical phonon mode around 300 cm^{-1} and Si–Ge mode around 420 cm^{-1}. The Ge–Ge optical mode mainly arises from the Ge dots rather than the Ge wetting layers, and it is much stronger than the second order transverse acoustic phonon mode for Si at 303 cm^{-1} [9]. Si–Ge mode implies the formation of SiGe alloy in the wetting layers. Lots of useful information can be obtained from these two peaks. The degree of Si/Ge interface intermixing can be determined by the ratio between the two integrated peak intensity of Ge–Ge and Si–Ge optical phonons [11]. It is valuable for analyzing the composition in the QDs. The strain and phonon confinement in the samples can be estimated by the red- and blue-frequency shift of the Ge–Ge optical mode according to the Ge bulk optical mode at 300 cm^{-1} [10–12].

Several Raman scattering peaks were observed in the low frequency region, which were attributed to the folded acoustic phonons in the Ge QD SLs. It was successfully explained by the Rytov's elastic continuum model. And we found that these Raman peaks' intensity was closely related to the Ge and Si layer thickness and the periods of the Ge QD SLs [13].

3. Conclusion

Self-assembled Ge QD SLs were grown by a solid-source MBE system with the SK growth mode. PL and Raman scattering measurements were carried out. Si TO-PL peak and broad Ge dot PL peak were observed in PL spectra. The temperature dependence of the PL intensity has been reported and fitted, from which the characteristic temperature T_B can be obtained. And the height and the effective mass of electron of the QDs could be estimated through T_B. The Si–Ge and Ge–Ge optical phonon modes and folded acoustic phonon mode were found in the normal and low frequency region of the Raman spectra. The Si/Ge interface intermixing, strain and phonon confinement in the samples can be estimated from the Raman spectra.

Acknowledgements

The work in NJU was supported by the National Natural Science Foundation of China under Grant Nos. 90101021 and 60290084 and also in part supported by the National Science Fund for Distinguished Young Scholars under Grant No. 60225014. Yang gratefully acknowledges Yuhua Qu and Lifeng Bian of ISCAS for some help in PL measurements. The work in UCR was supported by DARPA through the Center for Nanoscale Innovation for Defense and Liu thanks Shawn Thomas and Qianghua Xie of Motorola for some TEM characterizations.

References

[1] T.C. Harman, P.J. Taylor, M.P. Walsh, B.E. LaForge, Science 297 (2002) 2229.
[2] K.L. Wang, J.L. Liu, G. Jin, J. Cryst. Growth 237 (2002) 1892.
[3] G. Jin, J.L. Liu, K.L. Wang, Appl. Phys. Lett. 83 (2003) 2847.
[4] G. Abstreiter, P. Schittenhelm, C. Engel, E. Silveria, A. Zrenner, D. Meertens, W. Jäger, Semicond. Sci. Technol. 11 (1996) 1521.
[5] L.P. Rokhinson, D.C. Tsui, J.L. Benton, Y.H. Xie, Appl. Phys. Lett. 75 (1999) 2413.
[6] a J. Wan, G. Jin, Z.M. Jiang, Y.H. Luo, J.L. Liu, K.L. Wang, Appl. Phys. Lett. 78 (2001) 1763;
b J. Wan, G. Jin, Z.M. Jiang, Y.H. Luo, J.L. Liu, K.L. Wang, X.Z. Liao, J. Zou, Appl. Phys. Lett. 79 (2001) 1980.
[7] M.W. Dashiell, U. Denker, C. Müller, G. Costantini, C. Manzano, K. Kern, O.G. Schmidt, Appl. Phys. Lett. 80 (2002) 1279.
[8] a M. Kapoor, V.A. Singh, G.K. Johri, Phys. Rev., B 61 (2000) 1941;
b H. Rinnert, M. Vergnat, Physica, E, Low-Dimens. Syst. Nanostruct. 16 (2003) 382.
[9] a J.L. Liu, Y.S. Tang, K.L. Wang, T. Radetic, R. Gronsky, Appl. Phys. Lett. 74 (1999) 1863;
b A.V. Kolobov, K. Tanaka, Appl. Phys. Lett. 75 (1999) 3572;
c J.L. Liu, Y.S. Tang, K.L. Wang, Appl. Phys. Lett. 75 (1999) 3574.
[10] J.L. Liu, G. Jin, Y.S. Tang, Y.H. Luo, K.L. Wang, D.P. Yu, Appl. Phys. Lett. 76 (2000) 586.
[11] J.L. Liu, J. Wan, Z.M. Jiang, A. Khitun, K.L. Wang, D.P. Yu, J. Appl. Phys. 92 (2002) 6804.
[12] Z. Yang, Y. Shi, J.L. Liu, B. Yan, Z.X. Huang, L. Pu, Y.D. Zheng, K.L. Wang, Chin. Phys. Lett. 20 (2003) 2001.
[13] Z. Yang, Y. Shi, J.L. Liu, B. Yan, R. Zhong, Y.D. Zheng, K.L. Wang, unpublished results.